https://doi.org/10.33271/nvngu/2022-5/060

K. S. Zabolotnyi,
orcid.org/0000-0001-8431-0169,
O. L. Zhupiiev,
orcid.org/0000-0003-0531-2217,
V. V. Symonenko,
orcid.org/0000-0002-1843-1226

Dnipro University of Technology, Dnipro, Ukraine, e-mail: mmf@ua.fm

SUBSTANTIATING THE METHODS FOR CALCULATING THE SPLIT CYLINDRICAL DRUMS OF MINE HOISTING MACHINES WITH INCREASED ROPE CAPACITY

Purpose. A simplified calculation method development for strengthened split cylindrical drum structures of the mine hoisting machines of the TsR-6.75×6.2/1.95 type.

Methodology. The drum structure for the mine hoisting machines is conventionally divided into several nodes. A simplified averaged model is constructed for the nodes consisting of the shell, frontal, rib strengthening and brake discs (end nodes) based on the analysis of their operation, in particular, the stiffness analysis under different loads. After that, when assembling, the initial drum nodes are replaced with simplified ones and a so-called "simplified" model for the whole drum is constructed, as well as the displacements of the brake disc edges are determined.

Findings. The simplified models for drum nodes have been created based on the analysis of their operation, and then the displacements of the whole drum simplified model have been calculated.

Originality. The simplified calculation method error has been estimated: the method of averaging with increased thickness of the frontals.

Practical value. For the TsR-6.75×6.2/1.95 hoisting machine with a drum diameter of 6750 mm, a drum width of 6200 mm and an adjustable part width of 1950 mm, with a groove cutting pitch of 51 mm and a maximum lifting depth of 1477 m, it has been determined that the maximum axial displacements for brake disc edges of the jammed and adjustable parts are 0.854 and 1.921 mm, respectively. A simplified calculation method has been developed for strengthened split cylindrical drum structures of the mine hoisting machines of the TsR-6.75×6.2/1.95 type, available for use in middle-class packages such as SolidWorks Simulation.

Keywords: *method of averaging, axial stiffness, hoisting machine drum, strengthening with gussets and ribs, disc brake, thickened gussets*

Introduction. Due to the need to increase the depth of lifting the mineral and the associated increase in the size of the hoisting machine drum, as well as the complication of its structure, the calculation of axial displacements of the brake discs for the possibility of using disc brakes leads to the fact that the value of the finite element mesh becomes unavailable for the use of average level automatic design means.

Unsolved aspects of the problem. Due to the need to increase the lifting depth and the associated complication of the drum structure, the calculation of axial displacements of the brake discs for the possibility of using disc brakes requires the development of methods for calculating the hoisting machine drum in terms of axial stiffness based on the analysis of the operation of individual nodes, as well as the creation of their simplified models and the calculation of the drum model displacements with the subsequent calculation of stresses in the initial nodes. Finite element calculation on an acceptable quality mesh requires the use of high-performance PC and expensive software packages such as CATIA 5. This leads to the development of the latest methods for calculating such structures, available for use in middle-class packages such as SolidWorks Simulation.

Research purpose is to assess the application of the averaging method for calculating the hoisting machine drum of a complicated structure.

Literature review. The research works related to the development of hoisting and transporting machines are carried out at the National Technical University "Dniprovska Polytechnic". In this regard, scientists substantiate the structural and kinematic scheme of infinitely variable transmission [1], offer an innovative approach to the development of a hydraulic-mechanical transmission of a mine diesel locomotive [2]. In addition, for the first time, mathematical models for dynamic processes occurring in the haul truck engine under extreme conditions have been developed [3]. The vibrating feeder stressed state under push loading has been studied [4]. The scientific research results in the field of mechanics of new mine hoisting machine structures are also of great practical importance. Other studies are devoted to determining the dependence of dynamic parameters on the technical state parameters of the individual units in the installation [5].

Studies [6, 7] are devoted to the development and improvement of electromechanical equipment at mining enterprises, and studies [8, 9] deal with the problem of implementing heat pump technologies at mining enterprises.

Mathematical models have been developed that describe the frictional properties of mechanical systems [10], as well as the influence of thermophysical processes on the frictional properties of mechanical systems [11], taking into account the distributed and lumped parameters during stationary and non-stationary linear motion. The results of research on the development of methods for optimizing the drive parameters of mine diesel locomotives with increased traction-braking properties make it possible to develop a new generation of mining equipment [12–14].

The following scientists, such as B. A. Morozov, B. G. Klimov, B. I. Davidov, B. S. Kowalski, Z. M. Fedorova, A. P. Nesterov, F. L. Shevchenko, S. M. Zinchenko, K. S. Zabolotnyi, M. A. Rutkovsky were engaged in research on hoisting machines. Almost all the works of these scientists are devoted to the study on stresses in the drum elements of mine hoisting machines (MHM).

Scientific works, the analysis of which is given in [15], are devoted to the development of scientific methods for substantiating the design parameters of mine hoisting machines. The authors dealt with the following issues: braking devices on its stress-strain state (SSS) [16], developing a method for calculating the design loads [17]. They were ingaged into increasing the rope capacity of a single-drum mine hoisting installation [18], as well as substantiating the parameters of equipment for dehy-

dration of ropes in mine hoisting installations [19]. In addition, the method for calculating the force factors in the turns of multilayer winding of rubber-cable ropes has been improved [20].

In the work, a semi-empirical approach has been developed, which leads to obtaining a simpler analytical mathematical model of an object that provides reliable results. With this approach, the object is described through a simplified model, which uses coefficients determined experimentally and selected in such a way that, in this range of parameter changes, the calculated and experimental data are in good agreement. However, when determining the axial displacements of the braking fields caused by the own weight of the drum and the tension of the ropes, which run off and run on, the analytical method is not suitable and it becomes necessary to develop a specialized computational approach.

We use the method for calculating multilayer composite structures developed by V. V. Bolotin and Yu. M. Novichkov: 1) a simplified homogeneous model is studied with corresponding boundary conditions; 2) the SSS model is analyzed and the most stressed areas are selected; 3) the areas with the highest SSS are selected and boundary conditions for them are determined; 4) these areas from a homogeneous material are calculated and this material characteristics are determined; 5) a model from this material with specified boundary conditions is created and its calculation is performed; 6) the stresses are found at the boundaries of the selected areas and their calculation is performed for the real material.

The MHM drums belong to the class of thin-walled strengthened structures with elements of various thickness. This leads either to a large quantity of nodes with a mesh with a given maximum aspect ratio, or to a mesh with fewer nodes but a higher maximum aspect ratio. The MHM drums of a complicated structure are characterized by a large quantity of relatively thin strengthening elements.

The so-called "averaging method" has been widely used in solving the problems of celestial mechanics, whose main technique is that the right-hand sides of complex differential equations are replaced with "smoothed", averaged functions that do not contain rapidly changing system parameters.

In the statics and dynamics of ribbed shells, this method was used by I. V. Andrianov, V. A. Lesnichaya and L. I. Manevich.

When calculating complex structures such as aircraft fuselages and ship hulls, numerous solution methods that are economical in terms of machine time and resources should always use information about the analytical nature of the task.

Structural anisotropy schemes have been widely used in engineering calculations, according to which the initial shell is replaced with a smooth one with some of the specified parameters.

Inhomogeneities of the design or structure of the material are usually repetitive, periodic; therefore, valuable information about the system behavior can be obtained by replacing it with a simpler one with some of the specified (averaged) characteristics, which is typical when changing to structural orthotropy scheme. In this case, correct information can be obtained about such global characteristics as frequencies of vibrations or displacements, local ones such as stresses, determined with a large error. At the same time, the very determination of these parameters is a non-trivial task.

The essence of using the averaging method in structural mechanics can be briefly described by the following algorithm: 1. The initial structure is presented in the form of a set of nodes that allow a priori representation of their load and SSS. 2. The averaging parameter is chosen, usually the thickness of the shell or frontal, etc. 3. Parametric models of each such node are constructed. 4. Typical calculation cases are selected for all nodes, for example for strengthened drums – this is an axially-symmetrical compression or bending of the drum as a beam. 5. The values of optimization parameters are determined for each node, at which the averaged node stiffness in the selected calculation case of loading coincides with the initial strengthened node stiffness. 6. For each calculation case of loading the strengthened structure, an assembly is performed from the corresponding averaged nodes. 7. The calculations are compared and the most dangerous one is chosen.

Selecting the boundary conditions and calculating the initial model for the TsR-6.75×6.2/1.95 mine hoisting machine drum. A distinctive peculiarity of the studied drums is that they consist of two jammed parts and one adjustable part. This drum has two shells, six frontals strengthened with gussets and ribs, six frames, two bearing ribs, two brake discs, a shaft with hubs and two spherical double-row roller bearings (Fig. 1). To develop a calculation method, the drum is presented as a structure consisting of ten nodes.

In the studied drum structure, two spherical two-row bearings are used, which provide the possibility of shaft rotation in three directions and prevent its vertical displacement.

When calculating the radial stiffness of the bearings, we neglect the concentrated forces of the winding and twisting ropes, and take into account only the weight of the drum with the rope, equal to 2,207 kN.

$$P_C = P_d + P_r = 2207,$$

where P_d = 2049.3 is drum weight, kN; $P_r = H \cdot m_{run} \cdot g$ = = 1157.9 kN is rope weight; H is lifting height, m; m_{run} is mass of running meter of rope, kg; g is free fall acceleration, m/s^2.

It is proposed that eight rollers work in contact; therefore, one-eighth of the load on the bearing is used to calculate the FEM F_{lif1} = 137.9 kN.

Load acting on the bearing roller is

$$q = F_{lif1}/\text{h} = 7.45 \cdot 10^5,$$

where h = 185.1 mm is a bearing roller length.

For the analytical calculation of the bearing radial stiffness, one roller and the inner ring of the bearing are presented in the form of two cylinders with a diameter D_1, equal to 85 mm and D_2 equal to 847.5 mm. Fig. 2 shows a contact interaction scheme of the two cylinders. Undeformed cylinders with diameters D_1 and D_2 are shown by a dash-dotted line with two points.

The initial distance between axes of the cylinders is

$$L_1 = 0.5(D_1 + D_2) = 466.3.$$

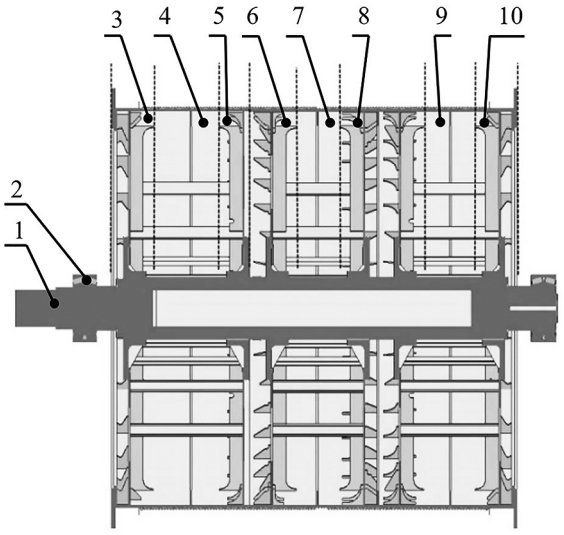

Fig. 1. Drum structure:

1 – a shaft with hubs; 2 – spherical bearing; 3 – left ring with gussets of the adjustable part; 4 – left ring of the shell with a rib; 5 – right ring with gussets of the adjustable part; 6 – left ring with gussets of the jammed part; 7 – ring of the shell with a rib; 8 – ring with two frontals; 9 – right ring of the shell with a rib; 10 – right ring with gussets of the jammed part

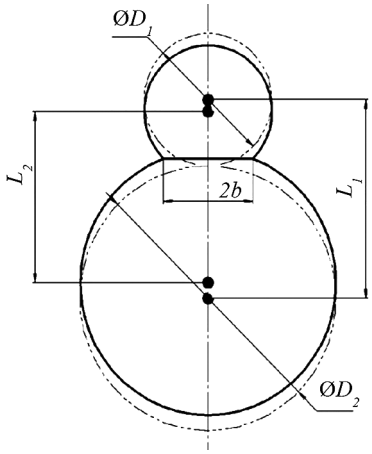

Fig. 2. Scheme of contact interaction of the roller and the inner ring of the bearing

A linear load q is applied to the first cylinder axis. The second cylinder axis is fixed. After applying the load, the cylinders converge, forming a flat contact surface $2B$ wide. The distance between the axes of the cylinders after deformation is denoted by L_2, and the convergence of the axes – by δ, which is equal to $\delta = L_1 - L_2$, mm

From the Hertz-Belyaev theory, the following expressions follow. Elastic constant of contacting bodies is

$$\mu = \frac{1-\vartheta_1^2}{E_1} + \frac{1-\vartheta_2^2}{E_2} = 8.9 \cdot 10^{-12}.$$

Contact strip half-width is

$$b = 1.128 \cdot \sqrt{\mu \cdot q \cdot 0.5 \cdot \frac{D_1 \cdot D_2}{D_1 + D_2}} = 0.571;$$

$$\delta = \frac{2 \cdot q}{\pi} \cdot \left[\frac{1-\vartheta_1^2}{E_1} \cdot \ln\left(\frac{D_1}{b} - 0.107 \right) + \right.$$

$$\left. + \frac{1-\vartheta_2^2}{E_2} \cdot \ln\left(\frac{D_2}{b} + 0.407 \right) \right] = 0.026,$$

where E_1, $E_2 = 2.1 \cdot 10^5$ are elastic moduli of the first and second bodies, MPa; ϑ_1, $\vartheta_2 = 0.25$ is Poisson's ratios of the first and second bodies; B is contact strip half-width.

Analytical stiffness of bearing nodes

$$C = F_{lift}/\delta = 5.284 \cdot 10^9.$$

Following the recommendations for self-aligning rolling bearings, the axial stiffness should be chosen equal to the radial stiffness.

As a parametric model of the bearing, the SolidWorks Simulation "Bearing support" tool is used.

The fourth, seventh and ninth drum nodes are rings, consisting of a shell with grooves and a rope, strengthened with a ring frame. As a model of these nodes, a homogeneous shell with equivalent stiffness is studied.

Since a shell is modelled by an axially-symmetrical model, it is sufficient to confine ourselves to a fragment limited in the circumferential direction by five degrees.

As a frame model, an initial structure is used, and to model a shell with grooves and rope, the following algorithm is applied.

With axial bending of a drum, three main areas can be distinguished: the upper one, in which tensile stresses predominate, the lower one – compressive stresses, and the middle one – with bending stresses. The boundary conditions for axially-symmetrical bending (Fig. 3, *a*) are chosen in the following form: the left side face of the shell is fixed relative to normal and radial displacements, and a radially directed force is applied to the right side face. As a calculation result, the average radial displacements of the right face can be determined.

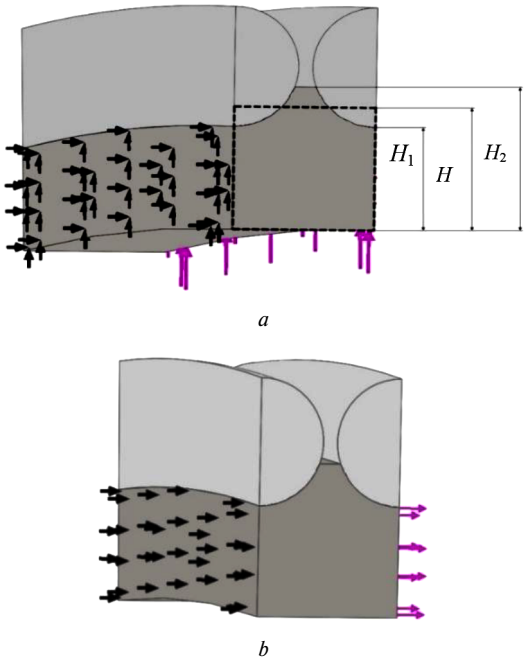

Fig. 3. Boundary conditions for axially-symmetrical bending (a) and for axially-symmetrical tension (b)

The axially-symmetrical tension is chosen as the second calculation case. The boundary conditions are shown in Fig. 3, *b*. The left face is fixed from axial displacements, and an axial force is applied to the right face. As a result of the calculation, the average axial displacement of the right face can be obtained.

The task set is to find a homogeneous shell thickness H in terms of axially-symmetrical bending.

The axially-symmetrical bending of a homogeneous shell with a thickness of H_1 and H_2 (along the bottom and tops of the grooves) is calculated. Then, the homogeneous shell thickness can be found from linear interpolation and a trial calculation can be performed. In the case, when the obtained values of radial displacements differ from the interpolation results by more than 10 %, an additional calculation should be performed with an averaged thickness between the thicknesses H_1 and H_2, and use quadratic interpolation.

For a shell with a rope in the case of axially-symmetrical bending of a fragment limited in the circumferential direction by five degrees, an average radial displacement of 0.001534 mm at a load of 1 MN can be obtained, and for axially-symmetrical tension – 0.000196 mm at a load of 10 kN. As a result of linear interpolation, the obtained thickness values are: H_{bend} is 44.53 and H_{tens} is 42.53 mm. The checking calculation gives an error in bending of 0.2 % (Fig. 4, *a*) and in tension – 0.22 % (Fig. 4, *b*).

For the calculation model, the shell thickness is taken to be equal to the smaller of the obtained thicknesses (42.53 mm).

In order to develop a calculation method that allows obtaining an acceptable result on a medium power computer, the drum was preliminarily calculated on a powerful computer, taking into account the mesh characteristics based on curvature. These characteristics are as follows: the maximum element size is 50 mm, the minimum element size is 10 mm, the total quantity of nodes is 3,352,229, the total elements are 1,874,904, the maximum aspect ratio is 11.26, the percentage of elements with an aspect ratio > 10–0.000213.

As boundary conditions, the loading of the drum by gravity, two tensile forces from the running off and running on ropes, as well as pressure from the wound rope, are studied.

Due to the small width of the gap between both parts of the drum (3 mm), the stiffness of the rope connecting these parts is neglected.

a

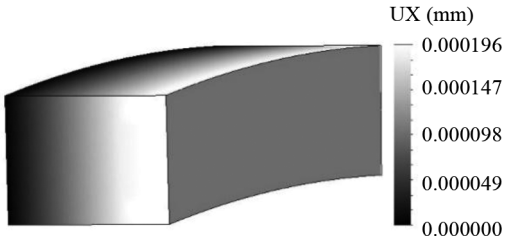

b

Fig. 4. Checking calculations of radial displacements in axially-symmetrical bending (a) and axial displacements in axially-symmetrical tension (b)

To reduce the resource intensity of the task, the halved tensile forces are applied not to the ropes, but to the underfaces formed by the section of the rope and the drum (Fig. 5). In addition, in order to eliminate the peculiarities of the resulting section figure, a rope is replaced with a body of square section.

The tensile forces from the running off and running on ropes are determined

$$T_2 = T_{\max} - 0.5 \cdot P_r = 371.1;$$

$$T_3 = T_{\min} + 0.5 \cdot P_r = 61.05,$$

where $T_{\min} = T_{\max} - T_{diff} = 140$ kN is minimum rope tension; $T_{diff} = 310$ kN is the difference in the tension of ropes.

At the same time, the angles of inclination to the horizon are 38 and 43° for the running off and running on ropes, respectively.

The distribution of pressure from the winding and rolling ropes is symmetrical with respect to the middle of the drum (Fig. 6).

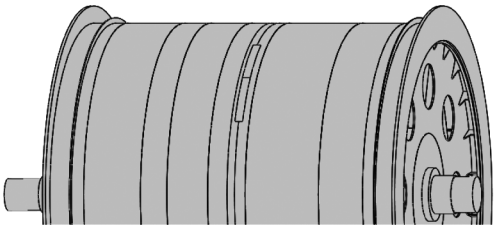

Fig. 5. Additional application of tensile forces to the underfaces

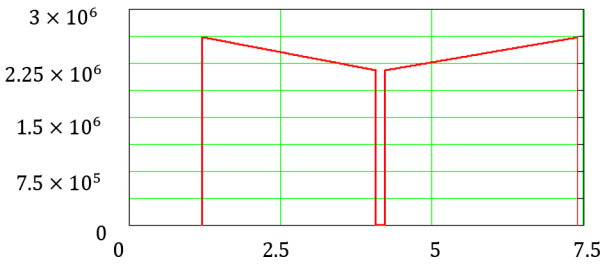

Fig. 6. Curve of the rope pressure distribution across the width of the drum

The following is taken in Fig. 6: $x_1 = 1.205$ m; $x_2 = 4.071$ m; $x_3 = 4.224$ m; $x_4 = 7.405$ m;

$$p_{ave} = \frac{T_{\max} - 0.25 \cdot P_{\hat{e}}}{R \cdot t} = 2.385 \cdot 10^6;$$

$$p_1 = p_4 = \frac{T_{\max}}{R \cdot t} = 2.614 \cdot 10^6;$$

$$p_2 = p_3 = \frac{T_2}{R \cdot t} = 2.156 \cdot 10^6,$$

where $T_{\max}$ is static rope tension, N; T_2 is static rope tension at points 2 and 3, N; R is a drum radius, mm; t is groove cutting pitch, mm.

The pressure from the wound rope should be set non-uniformly, since from the bearing rib to the middle of the drum (calculated case), the difference in pressure is provided by the wound rope weight. To take into account the nonuniformity, there are linear interpolation formulas

$$p(x) = \begin{cases} 2.385 \text{ MPa} \cdot (0.588 + 0.055 \text{ m}^{-1} \cdot x) & \text{if } x_3 \le x \le x_4 \\ 2.385 \text{ MPa} \cdot (1.067 - 0.061 \text{ m}^{-1} \cdot x) & \text{if } x_1 \le x \le x_2 \end{cases}.$$

Since the gravity force does not correspond to the initial model, it has been decided to change the density of the parametric model material

$$\rho_{simp} = m_{init} / V_{simp} = 9030.764.$$

According to the calculation results, it turns out that when loading from lifting a loaded skip from the right bearing rib (Fig. 7, *a*) of the drum, the maximum axial displacement values of the right and left edges of the brake discs are 0.854 and 1.921 mm, respectively.

The bearing rib is a thin-walled disk, which works on bending, and it is expedient to check its effect on the general deformed state of the assembly, since taking it into account leads to an increase in the quantity of nodes.

From the curve presented in Fig. 7, *b*, it can be seen that the bearing ribs do not have a great influence on the general deformed state.

In this case, the maximum axial displacement is 2.013 mm and the error is 4.8 %.

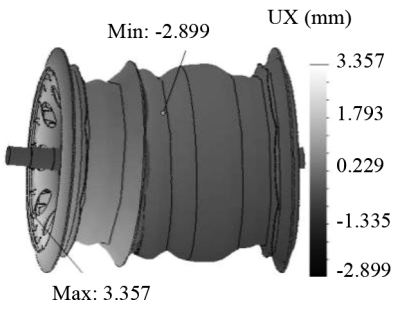

a

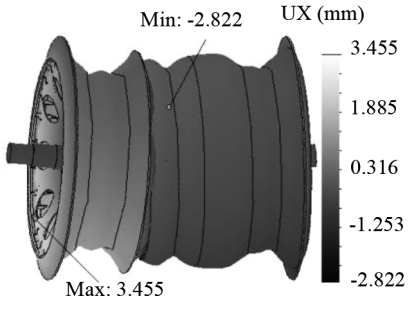

b

Fig. 7. Curve of axial displacements of the drum with bearing rib (a) and without bearing rib (b)

The averaging method application for calculating displacements of the TsR-6.75×6.2/1.95 hoisting machine drum. We illustrate the application of the method for calculating a particular hoisting machine.

Based on the averaging method algorithm, the drum structure is divided into ten nodes (Fig. 1).

It is unacceptable to select the shell thickness as an averaging parameter, since it is impossible to take into account the influence of ribs on the particular node behavior by changing this parameter. Therefore, the shell thickness is chosen equal to the initial one, and the influence of strengthening elements is taken into account by changing the frontal sheet thickness.

Based on the deformed shape analysis (Fig. 7) for nodes 3, 5, 6, 8 and 10, two calculation cases are chosen, such as shifting and loading with uniform external pressure.

As boundary conditions for the node model in the calculation case "shifting", its loading with a bending moment of uniformly distributed and oppositely directed forces on the end faces, equal to 1 mN, is studied. The frontal face is fixed in a place of its junction with a hub (Fig. 8, *a*). Boundary conditions for the calculation case "pressure" – the loading on the external cylindrical face of the shell with a pressure directed radially to the center, equal to 1 MPa. The face is fixed similarly to the preliminary calculation case (Fig. 8, *b*).

As an averaging parameter, the variable thickness of the frontal in the node structure without gussets and ribs is used (Fig. 9, *b*). To determine it, the difference between the average vertical displacements of the external right and left edges of the shell is used

$$\Delta = y_r - y_l,$$

where y_r and y_l are average vertical displacements of the external right and left edges of the shell.

In the first calculation, as the thickness b by the iteration method, the thickness of the frontal is chosen such that the difference in the average vertical displacements is greater than the difference in displacement for the initial node by 5–10 %. In the next two calculations, the thickness is increased by 5 mm in each case.

As a second calculation case, the load with an external pressure equal to 1 MPa is studied. The maximum radial displacement of the external edge of the node shell, located at the maximum distance from the frontal in the axial direction, serves as a parameter for determining the thickness of the frontal.

Similar to the calculation case "shifting", the frontal b thickness of the node 5 parametric model is found from the quadratic interpolation of three calculations.

Due to the inequality of the masses of the initial node structure and its parametric model, the subsequent calculation can give a large error. Therefore, the true density of the parametric node material for both calculation cases is determined from the formula

$$\rho_{simp} = m_{init}/V_{simp},$$

where m_{init} is weight of the initial node model, kg; V_{simp} is the volume of the parametric node model, m^3.

Node 6 differs from node 5 in that the gussets are located on both sides of the frontal. The boundary conditions for the calculated case of "shifting" are selected similarly to node 5. As a result of the calculation, the difference in the average vertical displacements of the end edges is determined. As the second calculation case, the load with an external pressure, equal to 1 MPa, is studied. Then, for each of the calculations, using quadratic interpolation, the rational thickness of the frontals can be found similarly to the previous node.

A distinctive peculiarity of node 8 is the high stiffness caused by the presence of two frontals. The parametric model is also projected with two frontals. As in the above cases, for the initial and parametric nodes, two calculations are made – "shifting" and "pressure", as well as the difference between the average vertical displacements and the maximum radial displacement, respectively, is determined. Then, for each of the calculations, using quadratic interpolation, the rational thicknesses of the frontals can be found similarly to the previous node.

Unlike the nodes studied above, node 3 has a bearing rib and a brake disc. The boundary conditions are similar to node 5, but the side face of the brake disc acts as one of the end faces. For the initial and parametric nodes, two calculations are made – "shifting" and "pressure" with the same boundary conditions as in the previous cases and the difference between the average vertical displacements and the maximum radial displacement, respectively, is determined. After that, for each of the calculations, using quadratic interpolation, the rational thicknesses of the frontals can be found similarly to the previous nodes.

Node 10 is a mirror image of node 3 and is modeled by the same model.

Aftewords, an assembly is created of a simplified model for the hoisting machine drum from parametric models of nodes 3–10, a shaft with hubs (node 1) (Fig. 10).

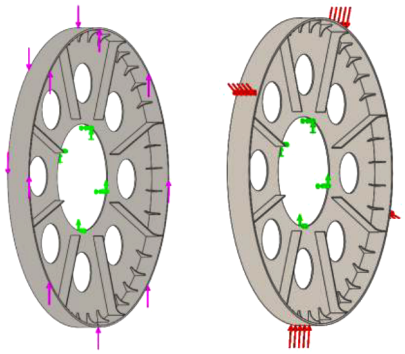

a *b*

Fig. 8. Boundary conditions for node 5 calculation:
a – calculation case "shifting"; b – calculation case of loading with uniform pressure

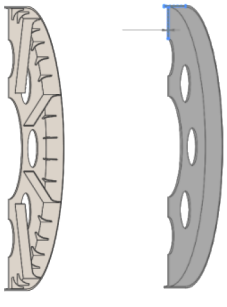

a *b*

Fig. 9. Node section 5:
a – initial tructure; b – parametric model

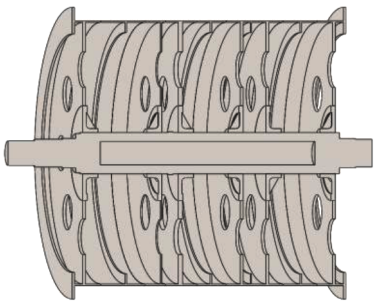

Fig. 10. Parametric model for the hoisting machine drum

Approbation of the developed method for determining the axial stiffness of the TsR-6.75×6.2/1.95 hoisting machine drum. As an example of a hoisting machine drum of a complicated structure, the TsR-6.75×6.2/1.95 hoisting machine drum is chosen, having strengthening in the form of 48 ribs, 224 gussets 20 mm thick, 48 gussets 16 mm thick and 64 gussets 14 mm thick.

Fig. 1 shows a general view of a single-rope single-engine hoisting machine with a cylindrical split drum of gearless design with single-layer winding.

Hoist type – skip-skip, lifting height is 1,477.657 m, drum diameter is 6,750 mm, jammed part width is 4250 mm, adjustable part width is 1,950 mm, maximum static rope tension is 450 kN, maximum rope tension difference is 310 kN, groove cutting pitch is 51 mm.

The drum consists of a jammed and adjustable parts, on which two running on and running off ropes are wound. There is a gap of 3 mm between these parts. Multi-strand steel rope "BRIDON" "Dyform" 34LR/PI (34×19), 46 mm in diameter is used.

The shaft is fixed in two spherical bearings 241/710. On the right side of the shaft, there is a cylindrical part for connecting to the drive.

Modeling of bearings is similar to the calculation of the initial drum model.

For the initial node 5, the difference in the average vertical displacements is equal to $\Delta = 7.21 - (-1.60) = 8.81$ mm (Fig. 11, *a*).

The frontal thickness is 38 mm and the corresponding difference in the maximum vertical displacements of the edges is 8.734 mm. In this case, the error, that is, the differrence between the differences in the average vertical displacements of the strengthened initial node and the parametric model, is 0.8 %. The checking calculation curve of the node 5 (calculation case "shifting") is shown in Fig. 11, *b*.

The parametric model density for the calculated case "shifting" is equal to 9,855.96 kg/m^3.

Similarly to node 5 for the calculation case "shifting", checking calculations are performed for nodes 6, 8 and 3(10), as well as the thickness values for the frontals of these nodes are determined (Table 1).

In Table 1, the letter δ_1 denotes the difference in the average vertical displacements of the initial node edges, mm; *s* is the frontal thickness in the averaged model, mm; δ_2 is the difference in the average vertical displacements of the average node model edges, mm; Δ is an error, %.

In this case, the material density for nodes 6, 8 and 3(10) is equal to 10470.39, 8280.21, 9126.06 kg/m^3, respectively.

For the initial node 5, the average radial displacement value is –1.749 mm (Fig. 12, *a*).

The frontal thickness in the averaged model is 36.284 mm and the corresponding maximum edge displacement is –1.748 mm. In this case, the error, that is, the difference in the maximum radial displacements of the initial strengthened node and the parametric model, is 0.06 %. The checking calculation curve of node 5 (calculation case "pressure") is shown in Fig. 12, *b*.

The parametric model density for the calculated case "pressure " is equal to 10051.68 kg/m^3.

Similarly to node 5 for the calculation case "pressure", checking calculations are performed for nodes 6, 8 and 3(10), as well as the thickness values for the frontals of these nodes are determined (Table 2). In this case, the material density for nodes 6, 8 and 3(10) is equal to 5196.19, 6689.91, 6941.43 kg/m^3, respectively.

In Table 2, the letter δ_3 denotes the maximum radial displacement of the initial node edge, mm; s is the averaged model frontal thickness, mm; δ_4 is the maximum radial displacement of the node averaged model edge, mm; Δ is an error, %.

Based on determined parameter values for models of each node, sketches of the corresponding rotation bodies are created, followed by cutting out eight symmetrically located holes in the frontal.

As a parametric model of a shaft with hubs (p. 1, Fig. 1), the initial structure of the node is chosen.

To create a finite element model of the drum, a medium-power computer is used, on which the calculation is limited by the quantity of finite element mesh nodes equal to 750,000.

As a result of creating finite element meshes, the resulting meshes based on curvature with a maximum element size of 100 mm for the calculation cases "shifting" and "pressure" have the following characteristics: for "shifting" case: quantity of nodes is 645,107; maximum aspect ratio is 23.547; for "pressure" case: quantity of nodes is 662,055, maximum aspect ratio is 23.422.

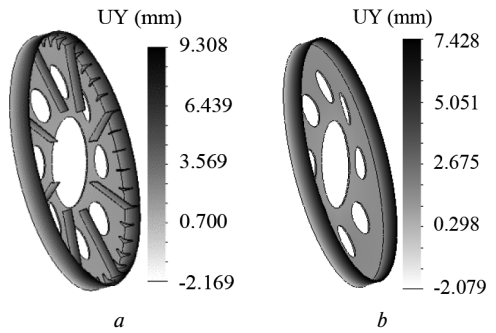

Fig. 11. Curve of the initial model vertical displacements (a) and checking calculation (b) of node 5

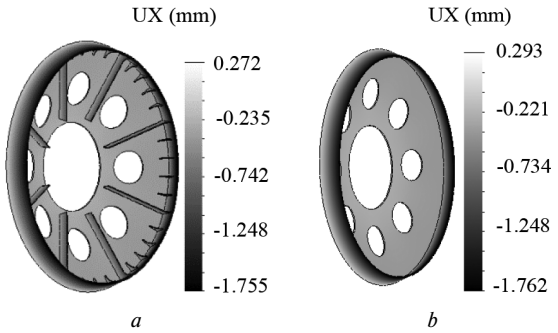

Fig. 12. Curve of the initial model radial displacements (a) and checking calculation (b) of node 5

Table 1

Thickness values for the frontals of the calculation case "shifting"

Node No.	δ_1	*s*	δ_2	Δ
5	8.807	38	8.734	0.8
6	16.617	39.374	16.665	0.3
8	1.231	55.174	1.230	0.08
3(10)	9.013	45.231	9.007	0.07

Table 2

Thickness values for the frontals of the calculation case "pressure"

Node No.	δ_3	*s*	δ_4	Δ
5	–1.749	36.284	–1.748	0.06
6	–1.048	109.444	–1.048	0
8	–1.078	75.416	–1.080	0.19
3(10)	–1.121	76.469	–1.121	0

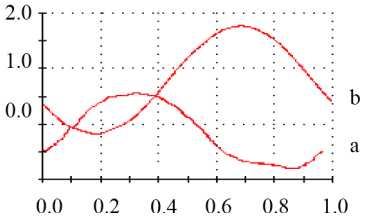

Fig. 13. Axial displacements of the drum brake disc edges in the computational case "shifting":

a – for the jammed part of the drum; b – for the adjustable part of the drum

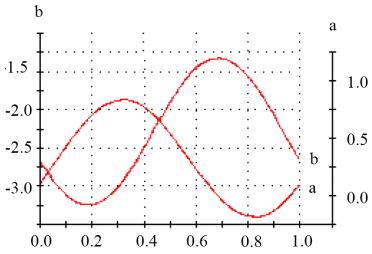

Fig. 14. Axial displacements of the drum brake disc edges in the computational case "pressure":

a – for the jammed part of the drum; b – for the adjustable part of the drum

The FFEPlus computer program is used for the calculation. Calculation time is 10.5 minutes.

As a result of the calculations, the axial displacements of the drum brake disc edges have been obtained:

- calculation case "shifting": for the jammed part (Fig. 13, *a*), the maximum positive value is 0.654 mm, the minimum negative value is 0.355 mm; for the adjustable part (Fig. 13, *b*), the maximum positive value is 1.766 mm, the minimum negative value is 0.176 mm.

- calculation case "pressure": for the jammed part (Fig. 14, *a*), the maximum positive value is 0.584 mm, the minimum negative value is 0.433 mm; for the adjustable part (Fig. 14, *b*), the maximum negative value is 1.327 mm, the minimum negative value is 3.246 mm.

The maximum error for "shifting" case is 8.1 %, for "pressure" case it is 69 %.

Conclusion by the averaging method with a change in the thickness of the frontals. In the averaging method, an important role is played by the choice of the so-called trial load, which is loaded on a separate element (node) of the structure with the selected fixing method. Thus, for the studied structures of drum nodes, two types of loading have been chosen: uniform external pressure and shifting during fixing the nodes along the border of their connection with the hub. Then the frontal thickness is determined, which provides the appropriate stiffness in the first and second cases. It has been revealed that the error of the maximum axial displacements of the brake disc edges is 8.1 % in the first case, and 69 % in the second case, when assembling from the nodes with averaged frontals. This indicates that, in fact, the nodes are exposed to a combined loading and, when using the first or second case separately, leads to an unacceptable error, which requires the development of other calculation methods.

References.

1. Samorodov, V., Bondarenko, A., Taran, I., & Klymenko, I. (2020). Power flows in a hydrostatic-mechanical transmission of a mining locomotive during the braking process. *Transport Problems, 15*(3), 17-28. https://doi.org/10.21307/tp-2020-030.

2. Sabraliev, N., Abzhapbarova, A., Nugymanova, G., Taran, I., & Zhanbirov, Z. (2019). Modern aspects of modeling of transport routes in Kazakhstan. *News of the Academy of Sciences of the Republic of Kazakhstan, 2*, 62-68. https://doi.org/10.32014/2019.2518-170X.39.

3. Naumov, V., Taran, I., Litvinova, Y., & Bauer, M. (2020). Optimizing resources of multimodal transport terminal for material flow service. *Sustainability, 12*, 6545. https://doi.org/10.3390/su12166545.

4. Nadutyi, V. P., Sukharyov, V. V., & Belyushyn, D. V. (2013). Determination of stress condition of vibrating feeder for ore drawing from the block under impact loads. *Metallurgical and Mining Industry*, *5*(1), 24-26.

5. Iljin, S., Samusya, V., Iljina, I., & Iljina, S. (2015). Influence of dynamic processes in mine winding plants on operating safety of shafts with broken geometry. *New Developments in Mining Engineering 2015: Theoretical and Practical Solutions of Mineral Resources Mining, 2015*, 425-429.

6. Trokhymets, M., Maltseva, V., Vialushkin, Y., Antonchik, V., Moskalova, T., & Polushyna, M. (2019). Method and equipment for the safe development of preparatory workings in the gas-bearing coal seams. *E3S Web Conferences*, (109). https://doi.org/10.1051/e3sconf/201910900102.

7. Kyrychenko, Y., Samusia, V., Kyrychenko, V., & Romanyukov, A. (2013). Experimental investigation of aero-hydroelastic instability parameters of the deep-water hydrohoist pipeline. *Middle-East Journal of Scientific Research*, *18*(4), 530-534.

8. Kyrychenko, E., Samusya, V., Kyrychenko, V., & Antonenko, A. (2015). Thermodynamics of multiphase flows in relation to the calculation of deep-water hydraulic hoisting. *New Developments in Mining Engineering: Theoretical and Practical Solutions of Mineral Resources Mining*, 305-311.

9. Pivnyak, G., Samusia, V., Oksen, Y., & Radiuk, M. (2015). Efficiency increase of heat pump technology for waste heat recovery in coal mines. *New Developments in Mining Engineering: Theoretical and Practical Solutions of Mineral Resources Mining*, 1-4.

10. Pivnyak, G., Samusia, V., Oksen, Y., & Radiuk, M. (2014). Parameters optimization of heat pump units in mining enterprises. *Progressive technologies of coal, coalbed methane and ores mining*, 19-24.

11. Ziborov, K., & Fedoriachenko, S. (2014). The frictional work in pair wheel-rail in case of different structural scheme of mining rolling stock. *Progressive Technologies of Coal, Coalbed Methane, and Ores Mining*, 529-535.

12. Ziborov, K. A., Protsiv, V. V., Fedoriachenko, S. O., & Verner, I. V. (2016). On Influence of Design Parameters of Mining Rail Transport on Safety Indicators. *Mechanics, Materials Science & Engineering*, *2*(1), 63-70. https://doi.org/10.13140/rg.2.1.2548.5841.

13. Ziborov, K., & Fedoriachenko, S. (2015). On influence of additional members' movability of mining vehicle on motion characteristics. *New Developments in Mining Engineering 2015: Theoretical and Practical Solutions of Mineral Resources Mining*, 237-241.

14. Protsiv, V., Ziborov, K., & Fedoriachenko, S. (2015). Test load envelope of semi – Premium O&G pipe coupling with bayonet locks. *New Developments in Mining Engineering 2015: Theoretical and Practical Solutions of Mineral Resources Mining*, 261-264.

15. Zabolotny, K., Zhupiev, O., & Molodchenko, A. (2015). Analysis of current trends in development of mine hoists design engineering. *New Developments in Mining Engineering 2015: Theoretical and Practical Solutions of Mineral Resources Mining*, 175-179.

16. Popescu, F. D., Radu, S. M., Andraş, A., Brînaş, I., Budilică, D. I., & Popescu, V. (2022). Comparative Analysis of Mine Shaft Hoisting Systems' Brake Temperature Using Finite Element Analysis (FEA). *Materials 2022*, *15*(9), 3363. https://doi.org/10.3390/ma15093363.

17. Zabolotnyi, K., Zhupiiev, O., & Molodchenko, A. (2017). Development of a model of contact shoe brake-drum interaction in the context of a mine hoisting machine. *Mining of Mineral Deposits, 11*(4), 38-45. https://doi.org/10.15407/mining11.04.038.

18. Ilin, S., Adorska, L., Pataraia, D., Samusia, V., Ilina, S., & Kholomeniuk, M. (2020). Control of technical state of mine hoisting installations. *E3S Web of Conferences, 2020, 168*, 00045. https://doi.org/10.1051/e3sconf/202016800045.

19. Zabolotny, K., Zinovyev, S., Zupiev, A., & Panchenko, E. (2015). Rationale for the parameters equipment for rope dehydration of mining hoisting installations. *New Developments in Mining Engineering 2015: Theoretical and Practical Solutions of Mineral Resources Mining*, 275-283.

20. Zabolotny, K., & Panchenko, E. (2010). Definition of rating loading in spires of multilayer winding of rubberrope cable. *New Techniques and Technologies in Mining – Proceedings of the School of Underground Mining*, 223-229. https://doi.org/10.1201/b11329-38.

Обґрунтування методики розрахунку розрізних циліндричних барабанів шахтних підіймальних машин збільшеної канатомісткості

К. С. Заболотний, О. Л. Жупієв, В. В. Симоненко

Національний технічний університет «Дніпровська політехніка», м. Дніпро, Україна, e-mail: mmf@ua.fm

Мета. Розробка методу спрощеного розрахунку підкріплених конструкцій розрізних циліндричних барабанів шахтних підіймальних машин типу ЦР-6,75×6,2/1,95.

Методика. Конструкція барабана шахтної підіймальної машини умовно поділяється на кілька вузлів. Для вузлів, що складаються з обичайки, лобовини, реберного підкріплення й тормозних дисків (крайні вузли), будується спрощена усереднена модель виходячи з аналізу його роботи, зокрема аналізу жорсткості при різному навантаженні. Потім у збірці вихідні вузли барабана замінюються на спрощені, збирається так звана «спрощена» модель усього барабана й визначається переміщення кромок гальмівних дисків.

Результати. Створені спрощені моделі вузлів барабана на підставі аналізу їхньої роботи, а потім здійснено розрахунок переміщень спрощеної моделі всього барабана.

Наукова новизна. Оцінена похибка методу спрощеного розрахунку: метод усереднення зі збільшеною товщиною лобовин.

Практична значимість. Для шахтної підіймальної машини ЦР-6.75х6,2/1,95 з діаметром барабана 6750 мм, шириною барабана 6200 мм і шириною переставної частини 1950 мм із кроком нарізання канавки 51 мм і максимальною глибиною підйому 1477 м встановлено, що максимальне осьове переміщення кромок гальмівних дисків заклиненої і переставної частини складають 0,854 и 1,921 мм відповідно. Розроблено спрощений метод розрахунку підкріплених конструкцій циліндричних розрізних барабанів машини типу ЦР-6,75х6.2/1,95, доступний для використання пакетів середнього класу типу SolidWorks Simulation.

Ключові слова: *метод усереднення, осьова жорсткість, барабан підйомної машини, підкріплення косинками та ребрами, дискове гальмо, потовщені косинки*

The manuscript was submitted 09.12.21.